Impact of the Packaging on the Static Behavior of Piezoresitive Pressure Sensor Dedicated to the Monitoring of Blast Waves

Bilel Achour, Lilian Marty, Kevin Sanchez, Samuel Charlot, Xavier Dollat, Benjamin Reig, Laurent Bouscayrol,
Aurélie Lecestre, Anthony Coustou, André Ferrand, Hervé Aubert, Patrick Pons

CNRS-LAAS, Toulouse University
Toulouse, France

E-mails: bachour@laas.fr, lmarty@laas.fr, ksanchezba@laas.fr, scharlot@laas.fr, xavier.dollat@laas.fr, breig@laas.fr,
laurent.bouscayrol@laas.fr, alecestre@laas.fr, acoustou@laas.fr, andre.ferrand@insa-toulouse.fr, aubert@laas.fr,
ppons@laas.fr

Abstract— The packaging is an important step, allowing to transform the transducer chip into a sensor. This step is necessary to perform the sensor characterization in a real environment, while minimizing the impact of the influence parameters on the sensor response. This study concerns the impact of the packaging on the static response of a miniature pressure sensor dedicated to the monitoring of blast waves. The transducer is based on 5 µm - thick rectangular (55 µm x 135 µm) silicon membrane and piezoresistive gauges. Pressure sensitivity measurements are performed using stressed and non-stressed sensor's holder configurations. Measurements results indicate that the pressure sensitivity is doubled when the sensor's holder is stressed. Finite Element Method simulations using COMSOL Multiphysics software show here that this result originates from the deformation of the sensor's holder, which leads to the deflection of the thin silicon membrane.

Keywords – blast waves; pressure sensor; packaging; mechanical stress; Finite Element Method.

I. INTRODUCTION

Shock waves are characterized by the propagation of a pressure discontinuity at supersonic speeds, which makes difficult the measurement of the overpressure peak [1]. For near-field experiments, the sensor's bandwidth required to ensure the accurate measurement of the overpressure is higher than 1 MHz [2]. To achieve such large bandwidths, the fundamental mechanical resonant frequency of pressure sensors must be far above 1 MHz (typically > 10 MHz).

However, the fundamental mechanical resonant frequency does not exceed a few MHz for commercial sensors dedicated to the monitoring of shock waves. To achieve higher mechanical resonant frequencies, studies focused on the design and fabrication of sensors using silicon or silicon dioxide micro-membranes with a lateral dimension of less than 100 µm and a thickness of a few microns [3]-[6]. However, the significant reduction of the membrane dimensions results in a very low sensitivity of the membrane deflection to applied pressure (typically, a few nm/bar). The measurement of such very small deflections is possible either from optical transduction [3]-[5], or by using strain gauges [6]. But the pressure sensor can be subjected to the deformation of its packaging, especially during dynamic characterizations [7]. Studies on high-bandwidth pressure sensors, published in open scientific Literature, generally do not address the impact of such deformation on sensor performances, whereas the experimental characterization of the sensors shows instabilities on the sensor's response after the passage of the shock wave front [3]-[6].

The work reported here aims to understand the impact of the packaging on the static response of piezoresistive pressure sensors dedicated to the monitoring of aerial shock waves. The obtained results will help us for the future design of optimized packaging dedicated to dynamic characterization of such sensors.

The paper is organised as follows. Section II is dedicated to the description of the pressure sensor, and Section III presents the experimental setup used for the static characterisation of the sensors. Measurement results are reported and analysed in Section IV. Mechanical simulation results are presented and discussed in Section V. Finally, the conclusion and perspectives of this work are drawn in Section VI.

II. PRESSURE SENSOR DESCRIPTION

The sensor is based on a rectangular silicon micro-membrane with 4 gauges located near its centre and connected in a Wheatstone bridge configuration (Figure 1). The manufacturing process of the sensor is detailed in [7]. The only difference with the design reported in [7] is the use of a Silicon-On-Insulator (SOI) substrate with 1 µm - thick buried silicon dioxide instead of a thickness of 2 µm. The main changes in the design relate to (see Figure 2): (a) lower access resistances to the Wheatstone bridge by defining the gauge length (P_+) by the distance between the heavily doped areas (P_{++}), (b) larger gauge size (2 µm × 10 µm instead of 1 µm × 5 µm) in order to reduce the impact of technological inaccuracies in the fabrication process, and finally (c) larger lateral dimensions of the membrane (55 µm × 135 µm instead of 40 µm × 100 µm) to compensate for larger gauge.
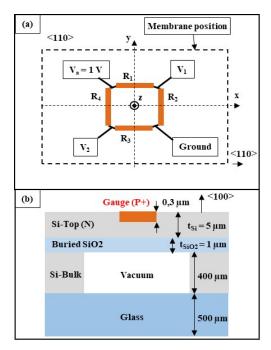
Figure 1. (a) Top view of the Wheatstone bridge reported on the membrane surface, (b) Cross sectional view of the transducer.
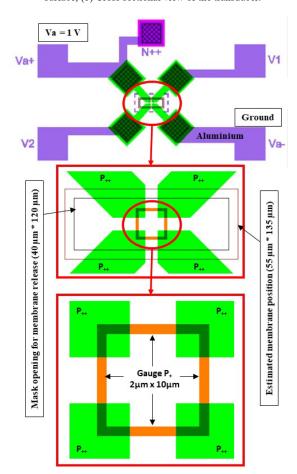
The theoretical fundamental mechanical resonant frequency F_0 of the membrane is about 10 MHz, that is, twice as low as the frequency reported in [7] but about 10 times higher than the fundamental resonant frequency of commercial sensors.

III. EXPERIMENTAL SET-UP FOR THE STATIC PRESSURE CALIBRATION

The setup used for the static calibration of pressure sensors is shown in Figure 3. The 4 mm - square silicon chip is glued on a 2.4 mm - thick stainless-steel holder using the thermosetting epoxy (Epotek-H70E) that is annealed for 90 minutes at 80°C. The device is then inserted into an airtight Static Pressure Box (SPB) connected to a pressure regulator (MENSOR APC600), which delivers a controlled relative pressure P_r ($P_r = P_{absolute} - P_{atmosphere}$). The pressure stability after regulation is ± 1 mbar. The sensor power supply ($V_a = 960$ mV ± 5 mV) is provided by the ELC- AL991S voltage generator. The differential output voltage V_s ($V_s = V_2 - V_1$) of the sensor is measured by using the Keithley-2000 multimeter with a resolution of 0.1 µV.

Figure 2. Top view of the mask used for the technological fabrication process (Purple / Green: Al / P++ interconnection, Orange: P+ Gauge)
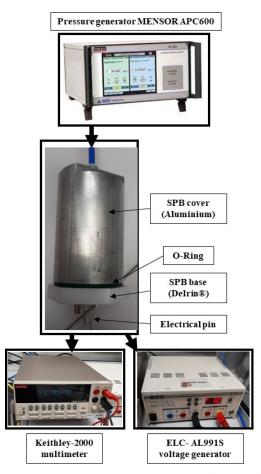

Figure 3. Experimental setup for the static pressure calibration of the sensor. (SPB: Sensor Pressure Box)

Two configurations are considered here to characterize the sensor:

i. Configuration #S: the sensor's holder is screwed onto the polymer (Derlin®) SPB base (Figure 4). The airtightness of the SPB is ensured by an O-ring (thickness ϕ_R = 2370 μm) embedded in the 1860 μm - depth groove. Before tightening process, the height of the O-ring protruding from the groove is therefore of 510 μm. The tightening of the screws is controlled by means of a 100 μm - thick calibrated metal wedge. The crushing of the O-ring is thus $\Delta\phi_R \cong 410$ μm (i.e. 17% of the initial thickness).

ii. Configuration #F: the sensor's holder is separated from the SPB base in order to reduce the stresses transferred to the sensor's holder (Figure 5). The airtightness of the SPB is then ensured by a holder without sensor, whose tightening is not controlled. The electrical connection between the two holders is achieved by using wires of about 5 cm long (the upper end is fitted with a female pin).
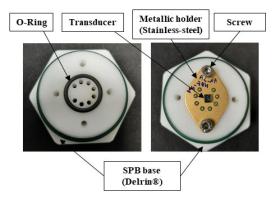
For both configurations #S and #F, the sensor pressure calibration is performed after a stabilisation phase, which takes at least 3 hours after the sensor placement inside the SPB. This phase is performed at atmospheric pressure and allows the mechanical relaxation of the sensor due to the stresses generated in holder. Next, the measurement of the voltage V_s is performed with increasing pressures, from the atmospheric pressure P_{atm} to a relative pressure P_r of 5 bar, with a step of 1 bar. The voltage V_s is measured about 2 minutes after the pressure stabilisation phase in order to achieve a good stability on V_s (± 10 μV). The voltage measurement for decreasing pressure is performed a few minutes after the first phase for which the pressure increases.

IV. MEASUREMENT OF THE SENSOR RESPONSE TO A STATIC PRESSURE

In Figure 6 to Figure 8 and Table I are displayed the measurement results for the two configurations (#S and #F) defined in Section III.

Figure 4. Configuration #S for the characterization of the sensor. (SPB: Sensor Pressure Box)
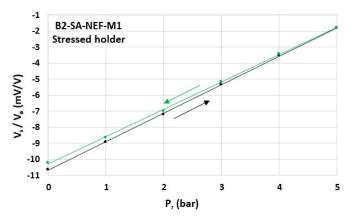

Figure 6. Sensor response in the configuration #S (Stressed holder).

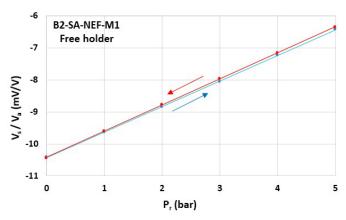Figure 5. Configuration #F for the characterization of the sensor. (SPB: Sensor Pressure Box)

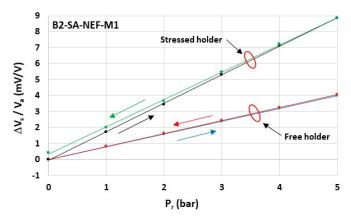Figure 7. Sensor response in configuration #F (Holder without stress).

Figure 8. Comparison of the sensor responses in both configurations. The voltage variation ΔV_s is normalized by the voltage V_s obtained before applying the increasing pressure.

TABLE I.   CHARACTERISITICS OF THE SENSOR RESPONSES

	Configuration #S (Stressed holder)	Configuration #F (Free holder)
Offset (Before applying the increasing pressure)	- 10.65 mV/V	- 10.42 mV/V
Offset (After applying the decreasing pressure)	- 10.21 mV/V	- 10.43 mV/V
Pressure sensitivity S_p (Increasing pressure)	1782 µV/V/bar	799 µV/V/bar
Pressure sensitivity S_p (Decreasing pressure)	1703 µV/V/bar	816 µV/V/bar

When the sensor's holder is not constrained (configuration #F), the magnitude of the pressure hysteresis is lower than the measurement accuracy (< 10 µV/V) and the pressure sensitivity S_p is between 799 µV/V/bar (for increasing pressure) and 816 µV/V/bar (for decreasing pressure). When the sensor's holder is constrained (configuration #S), the measurement results are less repeatable with a magnitude of the pressure hysteresis of 440 µV/V and a pressure sensitivity S_p ranging from 1782 µV/V/bar (for increasing pressure) to 1703 µV/V/bar (for decreasing pressure). This lower repeatability is probably related to partial stress relaxation in the sensor's holder during the pressure cycle. The stresses in the sensor's holder modify significantly the pressure sensitivity of the sensor (by a factor higher than 2).

V.   SIMULATION OF THE SENSOR RESPONSE TO A STATIC PRESSURE

In order to identify the origin of the large increase of the sensor's pressure sensitivity when the holder is constrained, mechanical simulations are performed by using COMSOL Multiphysics software (Finite Element Method) (Figure 9 and Figure 10). The 4 mm - square Silicon-Glass sensor chip described in Figure 1 is connected to the elliptical-shaped metallic holder with a 100 µm - thick glue (Young's modulus 8 GPa). We assume that the center of the metallic holder and membrane coincide and that the axis of the screws is along the membrane length. The O-ring (in blue in Figure 10) is modelled as a spring whose mechanical stiffness K_S is estimated at 174 N/mm from the measurement of the O-ring crushing (between 30 µm and 270 µm) for a given mass. The tightening force F_T of the screw is modelled by a force applied along the edge (in green in Figure 10) and is adjusted to obtain the desired crushing of the O-ring.
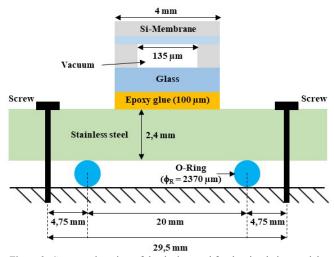

Figure 9. Cross section view of the device used for the simulation model.
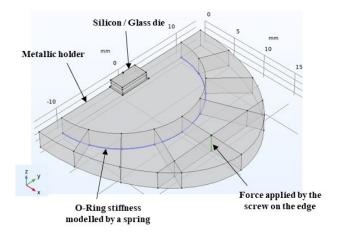

Figure 10. COMSOL 3D view of the half-simulated device. The membrane length is along x axis.

The pressure response of the device is simulated for four different cases, corresponding to different mechanical stresses on the sensor's holder (Figure 11). The case *#1* corresponds to configuration *#F,* in which the sensor's holder is not subjected to a mechanical stress, as the screw tightening force is zero and the pressure is identical at both sides of the sensor's holder. The case *#2* is associated with the configuration *#S,* in which the sensor's holder is subjected to two types of stresses that deform it, that is, (a) the differential pressure applied on the central part of the sensor's holder (inside the O-ring) and, (b) the screw tightening force. The cases *#3* and *#4* allow isolating respectively the effect of the differential pressure and the screw tightening force on the deformation of the sensor's holder (in case *#3*, the pressure is not applied to the membrane surface).
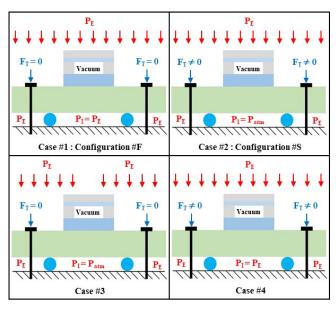

Figure 11. Description of the four studied simulation cases.

The simulations are performed with $P_E = 1$ bar absolute and $P_E = 2$ bar absolute. Table II shows the results obtained for the stress values at the centre of the membrane and at its surface. The stress extracted is the differential stress $\sigma_{xx} - \sigma_{yy}$, that is the stress along the length of the membrane minus the stress along its width. The pressure sensitivity S_p of the sensor is, as a first approximation, directly proportional to S_σ defined by the relationship (1).

$$S_\sigma = (\sigma_{xx} - \sigma_{yy})_{P_E = 2 \text{ bar}} - (\sigma_{xx} - \sigma_{yy})_{P_E = 1 \text{ bar}} \qquad (1)$$

TABLE II. SIMULATED STRESS ON THE SURFACE OF THE MEMBRANE AND FOR X = Y = 0 (CENTER OF THE MEMBRANE)

$\sigma_{xx} - \sigma_{yy}$	$P_E = 1$ bar	$P_E = 2$ bar	S_σ
Case #1 **(Configuration #F)**	2.86 MPa	5.72 MPa	2.86 MPa/bar
Case #2 **(Configuration #S)**	14.73 MPa	18.47 MPa	3.74 MPa/bar
Case #3	0	0.86 MPa	0.86 MPa/bar
Case #4	14.73 MPa	17.59 MPa	2.86 MPa/bar

The case *#1* provides the reference sensitivity of 2.86 MPa/bar, which corresponds to the sensitivity obtained when only the membrane deforms with the applied pressure. In this case, the offset ($P_E = 1$ bar absolute) is not zero since there is vacuum in the cavity below the membrane. When we add to case *#1* the tightening of the screws that deform the sensor's holder (case *#4*), the offset increases significantly ($\cong + 12$ MPa) but the pressure sensitivity is unchanged. The increase in pressure sensitivity (case *#2*) of 0.88 MPa/bar ($\cong +30\%$) comes from the deformation of the sensor's holder (case *#3*), which causes the deformation of the Silicon-Glass chip and in turn, of the membrane. These results are consistent with the measurement results, even if the simulated increase magnitude is much lower than the measured magnitude (30% instead of more than 100 %). More Multiphysics simulations would be necessary to identify the origin of this discrepancy.

Preliminary characterization is performed by increasing the thickness of the glass substrate (from 0.5 mm to 2 mm) in order to enhance the mechanical stiffness of the Silicon-Glass chip. Pressure measurements show an increase in pressure sensitivity of only 20% when moving from the configuration *#F* to the configuration *#S*.

VI. CONCLUSION

The development of new packaged sensors for the monitoring of blast waves is challenging. We have previously developed a transducer using silicon micro-membrane and piezoresistive gauges to reduce the reaction time compared to one achieved by commercial sensors and we have experimentally validated the dynamic behaviour of sensor using a shock tube. However, we identified undesirable effects, that lead to large drift after few microseconds.

In order to understand the impact of the packaging in the pressure sensor performances, we studied the sensor responses under static pressure and for various packaging configurations. Measurement results have shown that the sensor sensitivity to pressure is increased by more than 100% when the sensor's holder is deformed by applied pressure. Simulation results obtained from COMSOL software confirmed this effect (even if the simulated magnitude is not of 100%, but of 30% only) and indicated that it is related to the holder mechanical deformation

transferred to the silicon-glass die and to the membrane. The effect is large as the membrane deflection under pressure is very low (few nm/ bar). Preliminary characterizations with thicker glass substrate have shown a reduction by a factor six of the effect of holder deformation on the sensor pressure sensitivity.

In future works, the COMSOL model will be used to reduce the impact of the packaging on the dynamic responses of the pressure sensors to blast waves.

ACKNOWLEDGMENT

REFERENCES

[1] L. Walter, "Air-blast and the Science of Dynamic Pressure Measurements," Sound and Vibration, vol. 38, no. 12, pp. 10-17, December 2004.

[2] M. Chalnot, P. Pons, and H. Aubert, "Frequency Bandwidth of Pressure Sensors Dedicated to Blast Experiments," Sensors, vol. 22, no. 10, p. 3790, May 2022, https://doi.org/10.3390/s22103790.

[3] N. Wu et al., "Low-cost rapid miniature optical pressure sensors for blast wave measurements," Optic Express, vol. 19, no. 11, p. 10797, May 2011, doi: 10.1364/OE.19.010797.

[4] X. Zou et al., "Ultrafast Fabry–Perot fiber-optic pressure sensors for multimedia blast event measurements," Applied Optics, vol. 52, no. 6, p. 124820, February 2013, doi: 10.1364/AO.52.001248.

[5] C. Chu, J. Wang, and J. Qiu, "Miniature High-Frequency Response, High-Pressure-Range Dynamic Pressure Sensor Based on All-Silica Optical Fiber Fabry-Perot Cavity," IEEE Sensors Journal, vol. 21, no. 12, pp. 13296–13304, June 2021, doi: 10.1109/JSEN.2021.3068456.

[6] J. Riondet et al., "Shock Tube Characterization of Air Blast Pressure Sensor Based on Ultra-Miniature Silicon Membrane and Piezoresistive Gauges," Micro and Nano Engineering Conference, Turin, Italy, Sep. 2021.

[7] K. Sanchez et al., "Design, Fabrication and Characterization of a Novel Piezoresistive Pressure Sensor for Blast Waves Monitoring," International Conference on Sensor Device Technologies and Applications, Athens, Greece, Nov. 2021, pp. 47–52, ISSN: 2308-3514, ISBN: 978-1-61208-918-8.